Characterization of outcrop rock targets in Meridiani Planum using Pancam and Mini-TES spectra. L. A. Garchar[1] and W. M. Calvin[1], [1]Geological Sciences, MS 172, University of Nevada Reno, garcharl@unr.nevada.edu, wcalvin@unr.edu.

Introduction: Farrand et al. (2007) [1] identified two spectral units in the Burns formation based on the slopes of wavelengths from 482 to 535 nm in Pancam images. According to these findings, the buff-colored HFS unit is thought to contain iron-bearing minerals and be more oxidized, while the purple-colored LFS surfaces appear to be less oxidized. The HFS surfaces were interpreted to be weathering rinds, and LFS surfaces seem to reflect a fresher surface more exposed to aeolian erosion.

The goal of this research project is to assess a broad range of outcrop blocks where Pancam images and Mini-TES stares were taken concurrently, to see if the two sets of observations correlate. Preliminary analysis suggested that the LFS class contained a stronger hematite spectral signature in Mini-TES observations of Burns Cliff targets in Endurance crater and the Olympia region near Erebus crater [1].

For this project, we have focused on observations before sol 400, as later in the mission mirror dust complicates the appearance and interpretation of Mini-TES spectra [5]. To date, we have examined 11 rock targets with both Pancam and Mini-TES observations. This has included rock targets at Eagle, Fram and Endurance craters, specifically Shark's Tooth, Pilbara, Hamersley, Fuller, Escher, Sverdrup, Scoop, Aslan, Canidae, Bylot, and Ellesmere.

Methods and Observation: Pancam acquires data in 13 "Geology" filters at 11 unique wavelengths [1,2]. We used calibrated I/F images that represent surface reflectance [2]. Images of the rock targets were analyzed using color composites in both right and left eye filters using ENVI. It was found that the left eye filters were best at distinguishing subtle surface color variations. A decorrelation stretch (DCS) was performed on the left eye filters 3, 5, and 7 (L357) as red, green, and blue composite Pancam images. In addition to the buff/purple classes of Farrand et al. [1] we also noted numerous rock targets that had surface regions that were blue in the DCS and rock targets were classified as buff, purple, blue, or dusty according to their visual color. As an example of a target that includes both buff and purple classes, Pilbara from sol 85 is shown in Fig. 1.

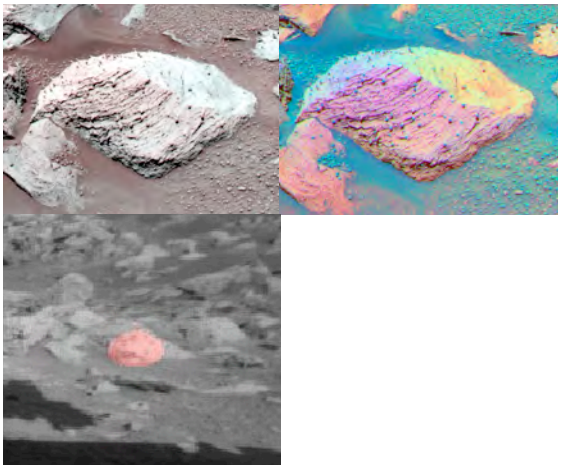

Figure 1. True color (left) and DCS (right) Pancam image of Pilbara shows both purple and buff classes. The Pancam image is sequence ID P2532. The red min-TES spot location (below) shows the targeting for sequence ID P3289 acquired on Sol 86 and shows that the stare is centered on the rock target.

Average Pancam reflectance spectra for the four color classes (buff, purple, blue, dusty), acquired on different outcrop blocks were calculated and plotted as a function of wavelength. These averages were created using a circular region of interest estimated to be about the size of a Mini-TES spot. The Pancam spectra were then scaled to 0.1 reflectance to minimize the varying albedo levels and to emphasize subtle slope and shape variations between the classes.

The spectral shape for hematite is a decreasing slope from ~760-810 nm and an increasing slope from ~910-1000 nm. The purple rock targets generally showed this characteristic bowl shape, indicating the presence of hematite. The buff and blue rock targets generally had more of a flat to down sloping shape in the ~760-1000 nm region. The dusty rock targets varied in spectral shape and there does not seem to be any common spectral profile associated with the dusty targets in the ~760-1000 nm region. Additionally, all color classes showed at least some spectral variability that may be due to lighting geometry as well as mixtures of different surfaces in the averaged spots. Representative Pancam spectra are shown in Fig. 2.

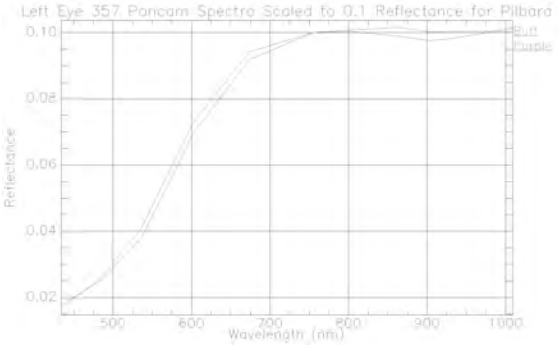

Figure 2. Purple spectra for Pilbara demonstrate a bowl shape on the right side of the graph, whereas the buff spectra show a flatter slope at wavelengths above 800nm.

For this study we restricted our analysis to those targets where Mini-TES had acquired long integration observations – "stares" of 200 individual spectral measurements averaged into a final spectrum. We used the emissivity product created by the instrument team [3] to compare spectra between rock color classes. Previous work had derived surface spectral end-members at Meridiani of basalt sand, outcrop, hematite, and a surface dust component, using a target transform (TT) approach [3]. Because no individual outcrop rock stare matches the shape of the target transform outcrop end-member, we modeled the data using linear deconvolution [4] in order to estimate the relative weight of surface components. Linear unmixing was performed using matrix calculation techniques created as custom IDL routines. This routine provides a fractional weight of the strength of an individual spectral component. Negative fractions are allowed, and are usually an indication of poor spectral fit using this simple set of end-members. Spectral fits, which are simply the sum of the fraction for each end-member multiplied by the end-member spectrum, were calculated for each Pancam rock target, as shown in Fig. 3.

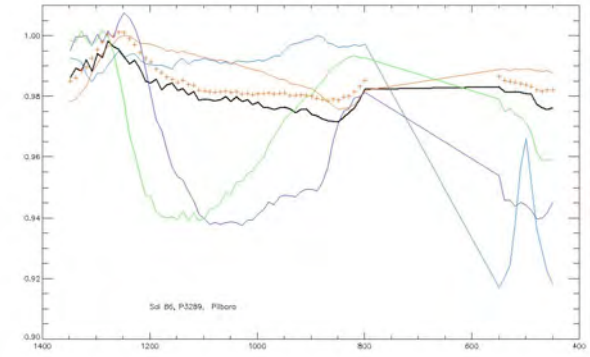

Figure 3. Single stare of Pilbara (black line) with TT end-members (colors) and fit (red plusses). TT end-members: outcrop (green), basalt sand (purple), hematite (blue), surface dust (red).

Initial Results: Unmixing for the Pilbara rock target fit the data with 0.78 dust, -0.03 hematite, 0.23 outcrop, and 0.13 basalt sand. The offset value -0.02 brings the spectral baseline down to match the observed spectrum. The spectral mismatches seen in Fig. 3 are noted in all cases. The model consistently overpredicts absolute emissivity values and does not match the magnitude of peaks and troughs in observed data. These spectral mismatches may be due to the limited end-member collection, or that the TT shapes don't represent the surface spectra well. An additional complication is that many surface stares of smaller blocks likely include a contribution from surrounding soils and so are not solely of the rock target alone.

To test the hypothesis that LFS blocks have a stronger hematite signature, we compared the strength of hematite features (determined by slopes between 469 cm^{-1} and 499 cm^{-1} and between 449 cm^{-1} and 529 cm^{-1}), the fraction of hematite returned by the unmixing program, and the Pancam derived color class. With these preliminary models, no correlation between these values and the DCS class of target was found. This mismatch is likely due both to the poor spectral fits using TT end-members and to inclusion of multiple surface components in the mini-TES spot. Images of the Mini-TES spots are being obtained from the MER Analyst's Notebook website to see how much of the rock target the outcrop stare includes, and to estimate the area percentage of surface components contributing to the stare using the Pancam images.

In order to test the range of spectral fits, additional unmixing using individual surface stares as end-members is currently underway. Surface derived end-members include a dune in Endurance crater, a bright patch on the rim of Eagle Crater, and an average of soil stares acquired throughout the mission for hematite [5]. Since no data of a pure surface outcrop has been identified, the original TT outcrop end-member is being retained.

Implications: The Pancam analysis conducted so far confirms findings of increased amounts of hematite in the purple rock class [1]. Mini-TES data unmixed with the new end-members may identify differences in spectral shape between the classes, but results are currently inconclusive. This information could offer further insight into the mineralogical composition of the outcrop and identify the presence of sulfates and their composition.

References: [1] Farrand et al. (2007). JGR, 112, E06S02, doi:10.1029/2006JE002773. [2] Bell et al. (2006) JGR 111, E02S03, doi:10.1029/2005JE002444. [3] Glotch et al. (2005). JGR, 111, E12S03, doi:10.1029/2005JE002672.. [4] Ramsey, M.S., Christensen, P.R. (1998). JGR, 103, no B1, pp 577-596. [5] Calvin et al. (2008). JGR, 113, E12S37, doi:10.1029/2007JE003048.